Proceedings of the 9th International Conference on Aluminium Alloys (2004)
Edited by J.F. Nie, A.J. Morton and B.C. Muddle

Modelling Dispersoid Precipitation and Recrystallization in Scandium and Zirconium Containing Aluminium Alloys

J. D. Robson, B. J. McKay, C. P. Heason

Manchester Materials Science Centre, Grosvenor Street, Manchester, M1 7HS, UK

Keywords: 7050, Hot rolled plate, dispersoids, recrystallization

Abstract

A model has been developed to predict the size, spacing, and distribution of the dispersoids in aluminium alloys containing zirconium and scandium. The model has been applied to predict the dispersoid pinning pressure in AA7050. The stored energy after deformation has been measured as a function of strain rate using EBSD. This, in combination with the calculated pinning pressure, has been used to predict recrystallization behaviour during solution treatment. These predictions have been compared to experimental observations.

1. Introduction

High strength aluminium alloys such as AA7050 contain zirconium to control recrystallization. This precipitates as Al_3Zr dispersoid particles that exert a pinning pressure on grain and subgrain boundaries. Since the dispersoids precipitate directly from the as-cast structure their distribution is very heterogeneous, reflecting the microsegregation of zirconium towards the centre of the dendrites [1]. This results in a variation in the recrystallization resistance, and where the dispersoids are sparse (towards the dendrite edges) undesirable partial recrystallization often occurs.

One method to reduce partial recrystallization is to add another dispersoid forming element, such as scandium, that segregates in the opposite direction to zirconium [2]. The presence of scandium leads to the formation of a ternary $Al_3(Sc,Zr)$ dispersoid phase [2]. Recently, a kinetic model has been developed to predict the precipitation and distribution of Al_3Zr [1], Al_3Sc [3] and $Al_3(Sc,Zr)$ [2] dispersoids. The model can be used to calculate the Zener pinning effect of the dispersoids as a function of position, composition and heat treatment. By comparing the variation in pinning pressure with the stored energy after deformation, the recrystallization behaviour can be predicted. This is demonstrated in this paper for AA7050 deformed over a range of strain rates.

2. Experimental

As cast 7050 ingot was provided by Alcoa Flat Rolled Products Europe. Specimens, approximately 10x10x50mm were cut and homogenized for 24h at 480^{o}C, followed by water quenching. Each specimen was then rapidly heated in a thermomechanical simulator (at the Alcoa Technical Centre, USA) to 450^{o}C, and compressed in a channel die

a total true strain of 1 at strain rates between 0.001 and 1. Following deformation, specimens were rapidly quenched, mechanically polished and electropolished at –30°C and 12V in a 70% nitric acid 30% methanol solution. Electron backscattered diffraction analysis was then performed in a high resolution field emission gun scanning electron microscope (FEGSEM), using a step size of 0.5μm. The results were analysed using the VMAP software package [4]. A portion of each specimen was then solution heat treatment for 1h at 480°C, overaged and etched using Graff-Sargents reagent (0.5% HF, 15.5% HNO_3, 84% H_20 3g CrO_3) to reveal the grain structure.

3. The Model

The model for dispersoid precipitation is outlined in Figure 1. There are two main components; a Scheil model to predict the initial distribution of the dispersoid forming alloying elements after casting, and a kinetics model, based on the Kampmann and Wagner numerical (N-model) approach [5] to predict the nucleation, growth and coarsening of the dispersoid particles. Details of the model are given elsewhere [1,2]. The outputs of this model are the dispersoid size distribution, volume fraction and number density as a function of position within each grain. This information provides the required parameters to predict the Zener pinning pressure due to the dispersoids.

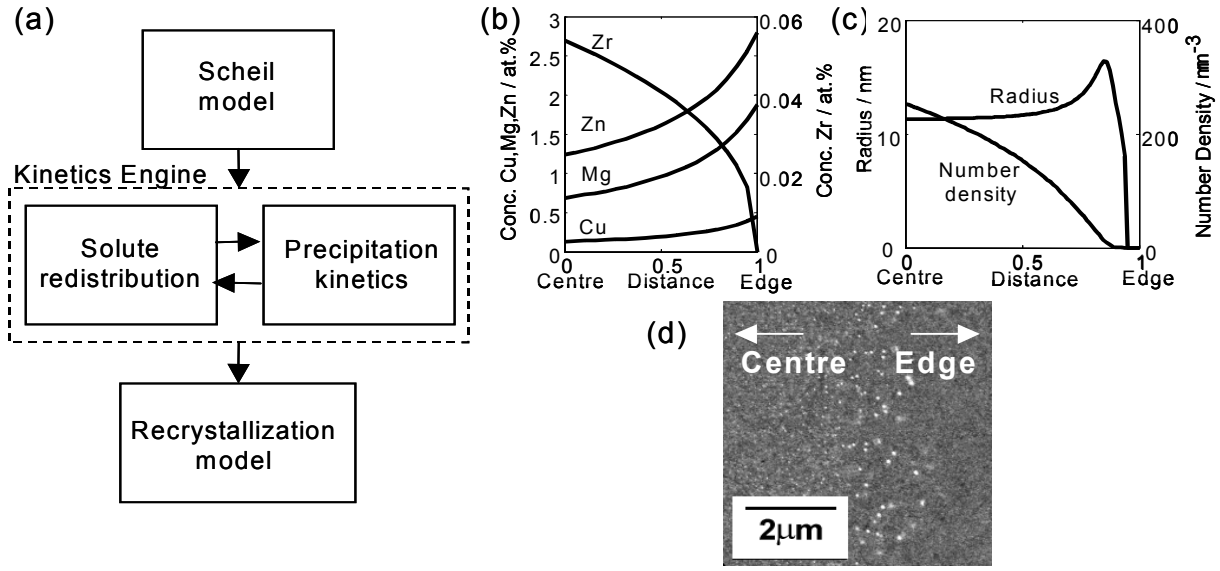

Figure 1: (a) Components of the model (b) Predicted variation in composition across a dendrite after casting using Scheil model for AA7050 (c) Example prediction of dispersoid size and radius across dendrite after homogenisation (d) FEGSEM image showing non-uniform dispersoid distribution within dendrites.

To predict the likely recrystallization behaviour during solution treatment, the dispersoid pinning pressure must be compared with the stored energy for recrystallization after deformation. Since the pinning pressure varies due to the non-uniform dispersoid distribution, there will generally be a region where the driving pressure for boundary migration due to the stored energy exceeds the pinning pressure. In these regions, boundary migration will be possible, and hence recrystallization may occur. In all other regions, the driving pressure for boundary migration will be insufficient to overcome the pinning effect of the dispersoids and recrystallization will not be possible.

The substructure after hot deformation of 7050 consists of subgrains, so the stored energy can be related to the subgrain size and misorientation. A region of material will be capable of recrystallising when the following relationship is satisfied [6].

$$\frac{3V_f\gamma_m}{r} < \frac{3\gamma_s}{D} \quad (1)$$

Where the left hand term represents the Zener pinning pressure (P_z) of the coherent dispersoid particles, with V_f the particle volume fraction, γ_m the energy of the boundary the particles are pinning, and r the particle radius. The right hand term represents the driving pressure for recrystallization (P_d), with γ_s the subgrain boundary energy (which depends on the subgrain misorientation [6]) and D the mean subgrain diameter. As a first approximation, it is assumed that the stored energy is uniformly distributed within the deformed grains. Therefore, the only factor that varies with position in equation 1 is the V_f / r ratio of the dispersoid particles.

4. Results

The dispersoid precipitation model has been validated against data for dispersoid precipitation in 7050 [1] and simple, model alloys (e.g. Al-Sc [2]). Examples of model predictions, each for a single concentration point, compared with experimental data are shown in Figure 2.

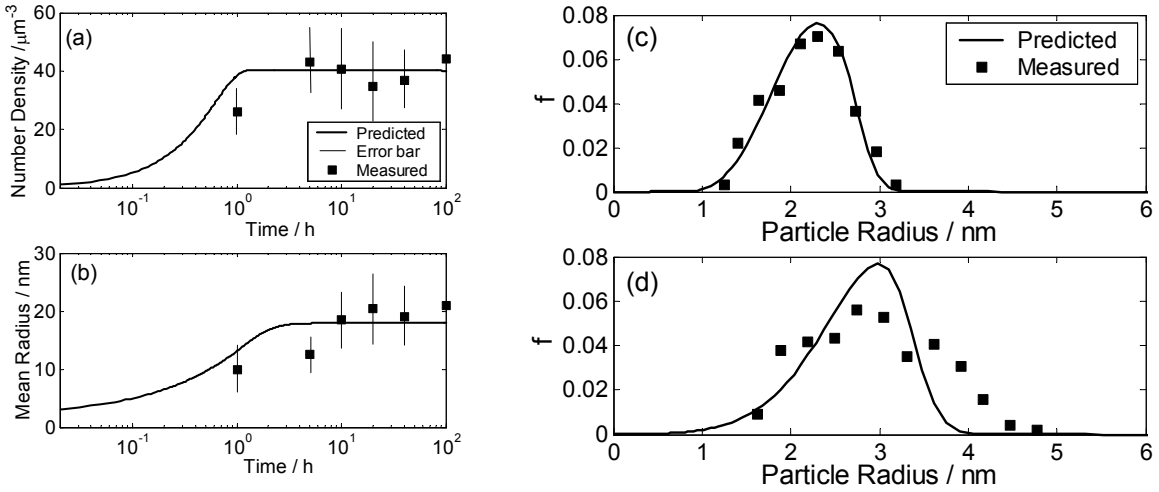

Figure 2: Predicted and measured [1] evolution of Al_3Zr in AA7050 at 500°C. (a) Number density and (b) radius. Predicted size distribution for Al_3Sc in an Al-0.3wt% Sc alloy aged at 300°C for (c) 6h and (d) 350h. Experimental data from Marquis and Seidman [7].

Once validated, the model can be used to predict the variation in dispersoid size, number and V_f / r ratio as a function of the distance across a dendrite (e.g. from centre to edge), alloy composition, and homogenisation treatment.

Figure 3 shows some example predictions of the dispersoid distribution across a dendrite after simulated homogenisation (24h at 480°C). Fig 3(a) is a plot demonstrating the predicted effect of small scandium additions to 7050 (0.13wt% Zr) on the size and number of dispersoids. A normalized distance of 1 corresponds to the dendrite edge, and 0 to the dendrite centre. In 7050 without scandium, the dispersoid number density falls to zero towards the dendrite edges, as a result of zirconium segregation. In addition, it is predicted that there is a band of large dispersoids adjacent to the dispersoid free zone. This has been confirmed experimentally [1].

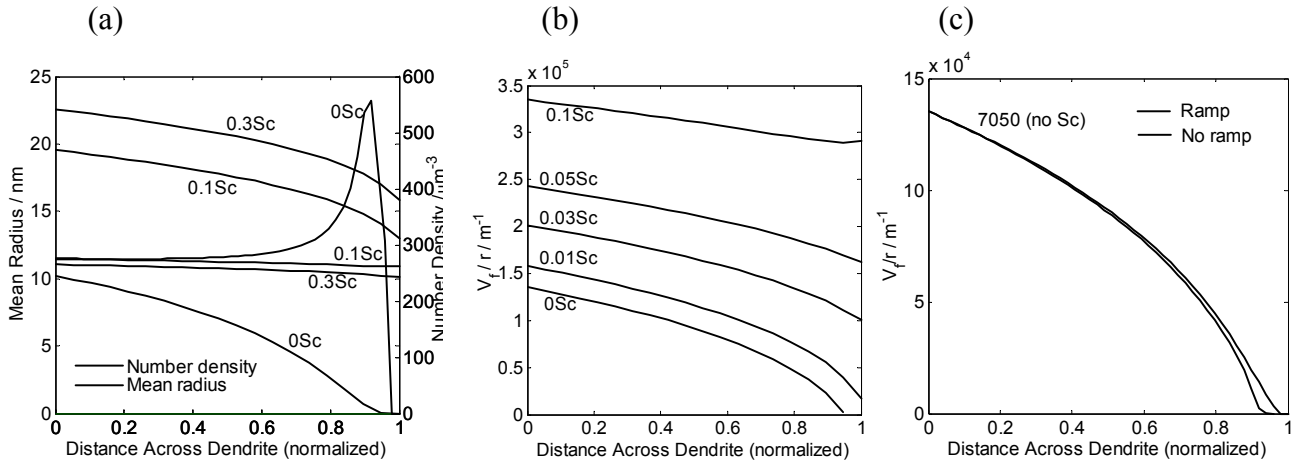

Figure 3 (a) Predicted variation in dispersoid size and number density across a dendrite (from centre to edge) after homogenisation for 24h at 480°C for 7050 (0.13wt% Zr) with 0.3wt% Sc, 0.1wt% Sc and without scandium. (b) predicted variation in the V_f/r ratio for 7050 with various scandium levels (all wt%) and the same homogenisation conditions. (c) predicted variation in the V_f/r ratio for 7050 without scandium, homogenized isothermally or with a 20h ramp heat up time to the homogenisation temperature (480°C)

Even a small addition of scandium is predicted to greatly boost the number density, particularly at the dendrite edges, where the local scandium concentration in enhanced due to segregation. Figure 3(b) shows the effect of scandium additions on the variation in the V_f / r ratio. Without scandium, this ratio falls to zero towards the edge of the dendrites, since there are no dispersoids present. This makes these regions particularly prone to recrystallization. Even very modest additions of scandium (e.g. 0.05wt%) are predicted to boost the V_f / r ratio towards the dendrite edges, so that it exceeds the value at the centre of the dendrites in alloys without scandium. Such an alloy is therefore predicted to have a greatly increased resistance to recrystallization. Experimental observations confirm the prediction that small scandium additions have a potent effect in suppressing recrystallization in 7050 [2]. Finally, Figure 3(c) shows the effect that slow heat up to homogenisation has on the V_f / r ratio in standard (scandium free) 7050. Slow heating is inevitable in the industrial homogenisation of thick ingots, and is predicted to have a small beneficial effect on the dispersoid distribution. This has been attributed to enhanced dispersoid nucleation during heating, particularly towards the dendrite edges where the zirconium concentration is at its lowest. The model provides a calculation of the pinning pressure. At present, it is not possible to calculate the stored energy directly for a complex industrial alloy such as 7050, which contains a mixture of large and small particles. Instead, the stored energy was derived from EBSD analysis of the substructure after deformation. Two typical EBSD maps are shown in Figure 4, corresponding to the two extremes of strain rate studied.

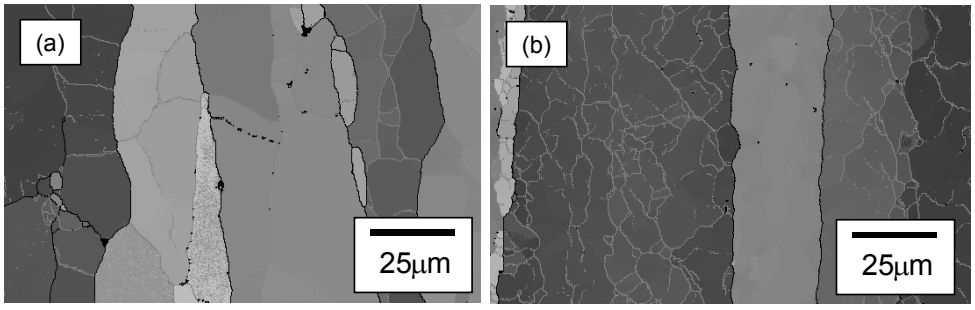

Figure 4 EBSD maps showing substructure after deformation at 450°C with a strain rate of (a) $0.001s^{-1}$, (b) $1s^{-1}$.

Mean subgrain sizes and misorientations were calculated from these EBSD maps. These were used to estimate the stored energy for recrystallization. The results are summarised in table 1. There was found to be a large range of subgrain size within each specimen, which leads to a large scatter in the averages and hence a large uncertainty in the stored energy.

Table 1 shows that both the subgrain size and misorientation increase as the strain rate decreases and hence the time available for dynamic recovery increases. It is noteworthy that over the range of conditions investigated, the subgrain size does not appear to be limited by the dispersoids (i.e it increases continuously as the strain rate is reduced). A calculation based on the average predicted V_f / r ratio gives an estimate of the average maximum dispersoid limited subgrain size ~15μm [6]. A value close to this limiting subgrain size is reached after deformation at the slowest strain rate ($0.001s^{-1}$).

From the predicted variation in V_f / r and the measured stored energies, the width of the region in which boundary migration is possible (i.e. where the driving pressure exceeds the pinning pressure) may be calculated. The calculated widths are shown in table 1. It can be seen that for samples deformed at a strain rate of less than 1, the width of the region where boundary migration is possible is less than the subgrain size after deformation. This suggests that further subgrain growth will not occur during solution treatment, and thus static recrystallization will not occur. Of course, this analysis is very crude, since it ignores the important effect of local variations in the subgrain size, and hence stored energy for recrystallization. Nevertheless, the prediction that boundary migration, and hence static recrystallization during solution treatment, will only be possible in the specimens deformed at a strain rate of 1 is consistent with experiment, as discussed below.

Table 1 Mean subgrain size (D), misorientation (θ) after deformation, calculated stored energy, predicted width of region where boundary migration is possible (pinning pressure less than driving pressure).

Strain Rate	D / mm	θ / °	Stored Energy /kJm^{-3}	Width of region where $P_z < P_d$ / μm
1	6.25	2.8	77	10.0
0.1	8.02	2.3	53	5.8
0.01	10.58	4.3	59	7.0
0.001	15.19	5	44	4.3

Figure 5 shows optical micrographs and EBSD maps after solution treatment for the two extremes of strain rate. Fig 5(b), which corresponds to deformation at a strain rate of 1, clearly shows recrystallised grains formed during solution treatment, surrounded by unrecrystallized regions containing a relatively fine substructure. In all other specimens (including that deformed at a strain rate of $0.001s^{-1}$, shown in Figure 5(a)), the structure consists of mainly unrecrystallized grains with a large mean subgrain size. The model predicts that the pinning pressure due to the dispersoids is sufficient to prevent these subgrains growing to form new recrystallised grains. These initial experimental observations are consistent with this prediction.

It is therefore possible to use to model to assess the likelihood of static recrystallization occurring during solution treatment for different alloy. For example, it is predicted that the addition of as little as 0.03wt% Sc to the 7050 alloy used in the present study (which contains 0.13wt% Zr) would be sufficient to give a pinning pressure that exceeds the driving force for precipitation at all positions, even after deformation at the highest strain rate investigated. This would be expected to completely suppress recrystallization.

5. Conclusions

A model has been produced to predict the precipitation kinetics of dispersoids in aluminium alloys containing scandium, zirconium, or both of these additions. The model is capable of predicting the dispersoid distribution that arises when precipitation occurs directly from a cast structure in which the alloying elements are segregated. The model has been used to predict the variation of Zener pinning due to the resultant non-uniform dispersoid distribution. Small scandium additions (<0.05wt%) to AA7050 (with 0.13wt% Zr) are predicted to very effective in enhancing dispersoid precipitation, and thus increasing recrystallization resistance, particularly towards the dendrite edges where zirconium is depleted, but scandium concentrated, due to segregation.

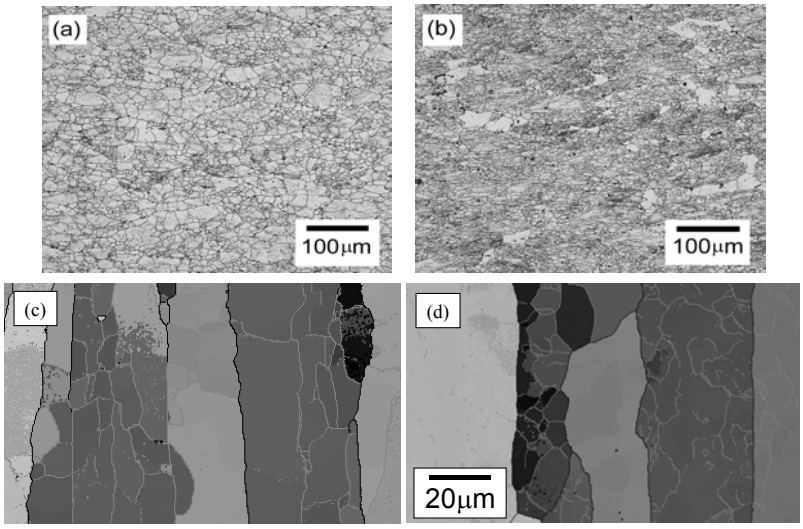

Figure 5 Micrographs and EBSD maps of etched solution treated specimens, deformed at 450^{o}C, strain rate (a,c) 0.001s^{-1}, (b,d) 1s^{-1}.

Deformation experiments on AA7050 show that as the strain rate of deformation decreases, the subgrain size and misorientation after deformation increase. This data has been used to calculate the stored energy, and hence the driving force for recrystallization. From this, and predictions of the pinning pressure, a simple model has been used to estimate the conditions for which static recrystallization is possible during solution treatment. Below a critical strain rate it is predicted that the driving force for recrystallization is insufficient to overcome the dispersoid pinning pressure and static recrystallization will not occur during solution treatment.

Acknowledgements

The authors are grateful to Alcoa for supporting this work. They would also like to thank Larry Lalli, Jaakko Suni and Ralph Shuey and Jacob Kallivayalil with the thermomechanical simulations

References

[1] J. D. Robson and P. B. Prangnell, Acta Mater. 49, 2001, p. 599
[2] J. D. Robson, Acta Mater. in press (corrected proof available online)
[3] J. D. Robson, M. J. Jones and P. B. Prangnell, Acta Mater. 51, 2003, p. 1453
[4] F. J. Humphreys, VMAP: Orientation Mapping and Quantitative Metallography by EBSD, UMIST, 2002
[5] R. Kampmann and R. Wagner, Materials Science and Technology vol. 5, VCH Weinheim, 1991
[6] F. Humphreys and M. Hatherly, Recystallization and Related Annealing Phenomena, Pegamon, 1996
[7] E. A. Marquis and D. N. Seidman, Acta Mater. 49, 2001, p. 1909